NTNU – Trondheim
Norwegian University of
Science and Technology

Axial flux machines with super high torque density or super high efficiency

Design Optimization of an Axial Flux
Permanent Magnet Machine Using Genetic
Optimization

Thomas Veflingstad

Master of Energy and Environmental Engineering
Submission date: July 2014
Supervisor: Robert Nilssen, ELKRAFT

Norwegian University of Science and Technology
Department of Electric Power Engineering

Design Optimization of an Axial Flux Permanent Magnet Machine Using Genetic Optimization

Thomas Veflingstad
Norwegian University of Science and Technology
Department of Electric Power Engineering
email: veflingstad.thomas@gmail.com

A challenge for electrical machinery is to compete with the hydraulic motors in applications where the torque densities required are beyond the capabilities if machines designed today. In order to build an electric machine capable of high torque densities, the geometrical dimensions must be small and the current densities must be high. Greenway Energy is developing an axial flux machine capable of delivering torque densities comparable to those of the hydraulic motor.

An analytical model of the axial flux permanent magnet machine developed by Greenway Energy is to be made. The model is to be optimized with Genetic Algorithms. Features for optimization with Genetic Algorithms, Gradient Based Optimizations Algorithms and hybrid solutions are available in MATLAB. The goal is to find a feasible, improved machine design using these optimization techniques.

Studies have been made to investigate the global search capabilities of stochastic optimization, like Genetic Algorithms, and local optimization capabilities of gradient based methods. A combination of stochastic optimization and gradient based optimization can be used to improve optimization of electrical machines.

A graphical user interface should be made to make the optimization tool easy to adjust and use. Constraints Through the user interface, constraints can be defined and the objection function can be changed. The most important results are displayed directly in the GUI, and additional results are displayed in the command window in MATLAB.

Supervisors:
Professor Robert Nilssen
PhD Jon Eirik Brennvall

Sammendrag

En analytisk modell av en aksial fluks permanent magnet maskin har blitt utviklet. Modellen er basert p en 2-D magnetisk krets beregnet p gjennomsnitlig radius med konstant magnetisk og elektrisk belastning. Modellen ble optimert ved hjelp av de innebygde funksjonene i MATLAB.

Optimeringsteknikkene Genetisk Algoritmer (GA) , GradientBasert Intern-Punkt optimering og en hybrid kombinasjon av de to metodene ble brukt til optimere modellen. Mlfunksjonene som ble optimert var totale matrialkostnad og totale livstidskostnad.

Den laveste gjennomsnitlige matrialkostnaden ble fundet ved hjelp av hybrid GA. Den laveste matrialkostnaden funnet var 58.86 % lavere enn kostnadene i det orginale designet. Virkningsgraden til denne maskinen var kun 13.7 % og effektfaktoren var 0.3.

Begrensninger ble satt p effektfaktoren for forbedre brukbarheten til optimeringsresultatene. Med en effektfaktorbegrensning p 0.85 ble et maskindesign funnet med en virkningsgrad p 33.3 % og matrialkostander 40.94% lavere enn opprinnelig.

Optimering med totale livstidskostnader kte virkningsgraden til 58.5 %. Matrialkostnadene til dette designet var 4.3 ganger hyere enn orginaldesignet, men totale livsstidskostnader var til gjengjeld 82.58 % lavere.

Et grafisk brukergrensesnitt har blitt laget gjennom GUIDE, MATLABs grafiske brukergrensesnittdesigner. Restriksjoner kan defineres av bruker direkte gjennom brukergrensesnittet og mlfunksjonen kan endres gjennom en drop-downmeny. De viktigste resultatene vises direkte i brukergrensesnittet, og dersom ytterligere resultater er nskelig vises disse i kommandovinduet til MATLAB.

Summary

An analytical model of an axial flux permanent magnet machine has been made. The model were based on a 2-D magnetic circuit calculated at average length assuming a constant magnetic and electric loading. The model were optimized using the built-in features in MATLAB.

Genetic Algorithms (GA), Gradient Based Interior-Point optimization and a hybrid combination of the two were used to optimize the design. The model were objective functions used were total material cost and total lifetime cost.

The lowest average material cost were found by using hybrid GA. The material cost of the cheapest design were 58.86 % lower than the original design. The efficiency of this solution was 13.7 % and the power factor was 0.3.

Constraints were put on the power factor to improve the optimization result. A machine design was then found with a 0.85 power factor, a 33.3 % efficiency and a material cost 40.94% lower than the original design.

Optimizing the design with regards to total lifetime cost increased the efficiency of the machine to 58.5 %. The material cost of the machine increased 4.3 times compared to the cheapest design, but the total lifetime energy cost of the machine was decreased 82.58 %.

A graphical user interface has been made for the optimizations by using GUIDE, MATLABs Graphical user interface designer. Through the user interface, constraints can be defined and the objection function can be changed. The most important results are displayed directly in the GUI, and additional results are displayed in the command window in MATLAB.

Design Optimization of an Axial Flux Permanent Magnet Machine Using Genetic Optimization

Thomas Veflingstad, *Student, Norwegian University of Science and Technology (NTNU)*

***Abstract*—An axial flux permanent magnet machine is being developed by Greenway Energy. AFPM torque production and potential topologies are presented. Previous work done on the machine design is summarized along with the description of the manufacturing, assembly and laboratory testing of a prototype. The strengths of the design is described. Iron is introduced to the design and relating problems are described. An analytical model of the axial flux machine has been made in MATLAB. The model has been run with Genetic Algorithm, Gradient Based Optimization and Hybrid Genetic Algorithm to find the optimization technique that gave the best result. Constraints were put on the performance of the machine to get more applicable results. Hybrid GA gave the best result with a 58.86 % reduction in machine cost. With a 0.85 lower limit to power factor, hybrid GA were able to find a design with 33.3 % and a 40.94% material cost reduction. The total lifetime energy loss were reduced by 82.58% when objective function was total lifetime cost. A graphical user interface has been made for the optimizations by using GUIDE, MATLABs graphical user interface designer. Through the user interface, constraints can be defined and the objection function can be changed.**

***Index Terms*—Genetic Algorithm, Optimization, Axial Flux Permanent Magnet Machine, Electrical Machine Design Optimization**

I. INTRODUCTION

THE earliest electrical machines were axial flux machines and the first prototype was built by M. Faraday in 1831[2]. However, the machine did not become the mainstream design for electrical machines because of fabrication difficulties, high costs and assembly difficulties.

Recent advances in axial flux permanent magnet (AFPM) technology the past 30 years have made AFPM machines feasible for use in a variety of applications where high torque density is required [3]. Different AFPM topologies have been thoroughly investigated in literature. Meanwhile, the cost of PMs has decreased while the maximum energy density of rare-earth magnets has steadily increased since its invention in the 1980s. High remrnance and demagnetization capabilities make it possible to replace the field windings in synchronous machines [1]. This results in a compact design with high efficiency and performance while still being economically viable.

China has recently gained a monopolistic position in rare-earth metal exporting. In 2011 the export decreased, leading to a shortage. Issues like these causes unstable price developments and are makes costs unpredictable. This affects AFPM machine costs because PM materials represent the largest contributor. This makes AFPM less viable and makes it harder for them to break through as the mainstream electric machine topology.

A. Background

The pursuit of cheaper electrical machines has always been important to be able to compete in the market. For every application there is a machine design that's both cheaper and better suited.

Several optimization methods are used to design electrical machines. Optimization methods can be categorized as either stochastic optimization or gradient based optimization. Tabu Search, Simulated Annealing, Genetic Algorithm (GA), Particle Swarm Optimization (PSO) and Differential Evolution are examples of Stochastic Algorithms. G) seems to be the most popular stochastic optimization method but PSO is an increasingly popular choice [29]. A study of the possibilities and limitations of gradient based optimization has been done in [30]. [29] investigates both a Genetic Algorithm and Particle Swarm Optimization and the effect of combining the two with Gradient Based Optimization to make hybrid solutions.

II. OPTIMIZATION METHODS IN MATLAB

Optimization tools find the best solution to an objective function that's within the lower boundaries and the upper boundaries of the independent variables. The solution must also meet the inequality constraints and the equality constraints set. A basic formulation of an optimization problem can be shown as [29]

$$\min_n F(X) \tag{1}$$

$$g_i(x) \leq b_i \tag{2}$$

$$h_j(x) = d_j \tag{3}$$

$$L \leq x \leq U \tag{4}$$

for i = 1 : p and j = 1 : q. g_i are the inequality constraints while h_j are equality constraints.

F(x) is the objective function that decides which aspect of the machine that will be optimized and the quality of each solution relative to each other. L the lower bounds while U is the upper bounds for the independent variables. The feasible solution space is defined the inequality constraints, the equality constraints and the lower and upper bounds.

The optimization used in this report are Genetic Algorithms alone and in combination with gradient based optimization.

MATLAB provides a complete package of Genetic Algorithm features in The Global Optimization Toolbox [39]. A function for gradient based optimization is also included in the tool box. The implementation of GA, Interior-Point and hybrid optimization by using the built-in features in MATLAB is shown in Appenix A.

A. Genetic Algorithms

Genetic Algorithms (GA) are stochastic optimization algorithms that mimics the behaviour of evolution to search through a vast solution space to find a solution that is as close to the global optimum as possible. The algorithms are also called evolution programs [40]. The can be visualized as follows:

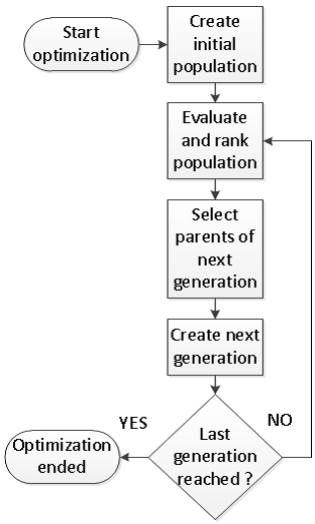

Fig. 1. Flow chart describing the process of Genetic Algorithms

An initial population of individuals are evaluated based on how good they are. Each individual represents a possible solution. The parents of the next generation are then chosen out of the population and a new generation is created. The process is then repeated with the exception of initializing a new population. When selecting the parents, several selection algorithms may be utilized together with genetic algorithms. *The tournament selection* was chosen based on the recommendations from [29]. This selection can't originally handle integer variables, but this was avoided by dividing these variables and their upper and lower bound by 10^3. The variables were multiplied by 10^3 in the model and rounded to the nearest integer with the MATLAB-function round().

The tournament selection hosts N number of tournament to decide N number of winners. The winners of these tournaments are the most fit individuals of the tournament contestants and will go on to create the next generation. This selection will give higher fitness values of each individual that will create the next generations. The new generation will in most cases also have higher fitness value, which in turn makes the algorithm converge on result faster. This selection will require more computer resources than the default selection.

When the new generation is created, genetic operators are utilized. *The crossover operator* combines one part of of one parents genes with one part of the other parents genes. *The mutation operator* randomly change one or more points in the genetic sequence of one individual. These operators are often applied after *the crossover operator* has made the new individuals. *An Elite operator* can be used to send the most fit individuals directly to the next generation as if they were cloned. This may help reaching the global optimum faster.

B. Hybrid optimization

Hybrid optimization is a combination of a stochastic optimization algorithm and a gradient based optimization algorithm. Stochastic optimization algorithms are good at finding the global optima without getting stuck in any local. However, the algorithm tends to converge too early without reaching the absolute optimum solution. Gradient Based Optimization methods requires a gradient to be able to search in the right direction and to know how far to move in that direction. They converge better, but are generally unable to escape local minima. The hybrid approach avoids these disadvantages and benefits of the advantages of both methods, giving a better result of the optimization.

The standard optimizer for constrained non-linear problems in MATLAB is *fmincon*. Through this function, 4 different gradient based algorithms can be implemented. These are; *Trust Region Reflective Algorithm*, *Active Set Algorithm*, *Interior Point Algorithm* and *SQP Algorithm*. Gradient based optimization are made for problems with continuous objective functions with continuous constraints and first derivatives. This implies that integer variables can't be used by *fmincin*. However, since GA is able to solve integer variables, this problem can be avoided by putting the upper and lower bounds of the integer variable equal to the answer found by GA before applying fmincon. By doing this, the integer variable will act as a constant when fmincon is running.

All four of the algorithms in *fmincon* were tested on a tidal generator model in [30]. Trust *Region Reflective Algorithm* would not be used on non-linear constraints. It is therefore not usable for electrical machine optimizing and out of the three remaining, applicable algorithms, *Interior points Algorithm* gave the fastest and most robust solution.

Interior Point Algorithm solves a problem as a sequence of approximate minimization problems by changing the inequality constraints into equality constraints [39], [29]. This is done by introducing slack variables that are added to each inequality. The problem was formulated in [29] as:

$$\min_{n,s} f_\mu(x) - \mu \sum_{i=1]} ln(s_i) \tag{5}$$

Subject to:

$$g(x) + s = 0 \tag{6}$$

$$h(x) = 0 \tag{7}$$

$$\mu \to 0 \Rightarrow f(x) \to f(x)^* \tag{8}$$

Where $\mu$is a constant and each s is a slack variables. The algorithm first tries to solve the problem with Direct step or Newton step. If this step fails, it then solves the problem with a Conjugate Gradient step by using a trust region approach [39].

A study of the design capabilities of Particle Swarm Algorhtms, Genetic Algorithms and hybrid solutions was done in master thesis of Erlend Engevik [ref Erlend]. The results from the investigation indicated that GA were generally able to find a better design than PSO. On average, GA with 25 individuals were able to find a design that were 19.1 % cheaper than PSO with 25 particles and 200 iterations. Hybrid GA performed better than regular GA, reducing the average cost of the problem with 31.2 %. Hybrid GA also showed better convergence, less variance and shorter computation time than its PSO counterpart. The solution found was 5.2 % lower and the variance was 98.6 % lower than the results hybrid PSO was able to find.

C. Parallel Processing

To increase the precision of the optimization, the number of independent variables, individuals and iterations can be increased. However, doing this will considerably increase the computation time and the resources needed. To be able to efficiently work with such problems, parallel processing can be applied. Parallel processing is to use more than one computer processor to perform work on a problem. By doing this, independent tasks are performed simultaneously, reducing the computation time drastically. This means that the problem must be made up of independent tasks. The number of tasks must also be large enough to defend the administration cost of distributing each task to an independent processing unit. For GA with 2500 individuals, the computation time was reduced from 12 hours to 21 minutes by using parallel processing with 48 processor cores [29]. Parallel processing for GA can be implemented in matlab by enablig 'UseParallel', 'always' in the options for the GA-function.

III. AXIAL FLUX PERMANENT MAGNET MACHINES

The produced by electromagnetic torque in electrical machines are given by equation (1):

$$\overrightarrow{F} = q\overrightarrow{v} \times \overrightarrow{B} \tag{9}$$

Where $\overrightarrow{F}$ is the magnetic field acting on the current $q\overrightarrow{v}$. The force, $\overrightarrow{F}$ is always acting in a circumferential direction in rotating electric machines. Because of this, the currents and the magnetic fields are confined to the radial and axial directions. This leads to the difference between radial and axial flux machines; the radial flux machine produce torque by means of radially directed magnetic flux, while axial flux machine establish axially directed magnetic flux.

The strength of an axial flux machine is the possibility to make a very compact, disc shaped motor with a very high torque to volume ratio, torque density. The radial flux machine can be scaled by adjusting the length of the machine, while the axial flux machine has an optimal machine length for a give diameter. This is shown by the torque sizing equations for the radial flux machine, (2), and the axial flux machine, (3).

$$T_{Radial} = kD^2L \tag{10}$$

$$T_{Axial} = kD^3 \tag{11}$$

Where k is the machine constant, which is used to compare machines with equal design, D is the diameter of the rotor and L is the axial length of the machine [3]. It is evident from these torque sizing equations that the radial flux machines are suitable for applications where the length of the machine is a trivial matter and axial flux machines are suited for applications where the diameter isnt an issue. Despite the fact that the torque is equal to the diameter cubed, the effect of increasing the diameter diminishes if the diameter to length ratio is too great [2]. To increase the torque beyond this point, multiple discs are stacked on the same shaft. Increasing the length of radial flux machines is more advantageous than stacking discs because the end coil volume remains the same. Each disc on the other hand, has the same amount of end coil which adds up when stacking the discs. Better cooling capabilities can however be expected in axial flux machines because the inner diameter of the core usually is much greater than the shaft diameter [2]. AFPM also has a planar air-gap that can be adjusted to some degree and greater outer diameter means that more poles can be accommodated.

A. AFPM topologies

A variety of topologies can potentially be used to produce torque from axial magnetic fields. There are advantages and disadvantages for each and every topology available. Only the disc machine topologies have been considered here.

The most fundamental of the disc topologies for AFPM's is *the single sided machine*. This arrangement consist of one rotor disc containing the magnets and one stator disc containing the coils. The magnets in the rotor alternates between having the north and the south pole facing the stator disc. Axially directed attractive forces between the rotor and the stator disc may cause the rotor disc to bend. Because of this, the rotor disc may require support or strengthening. The topology generally consist of few parts and offer a low cost, compact design despite the potential need of support, and topology is commercially used by the Finnish elevator company KONE, Inc.

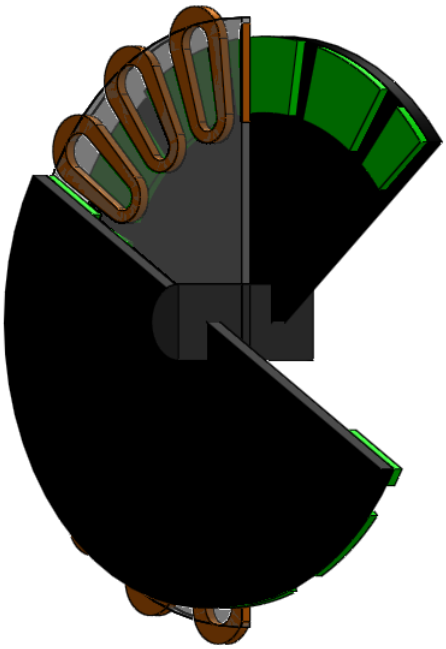

Fig. 2. Double sided internal stator AFPM from [1]

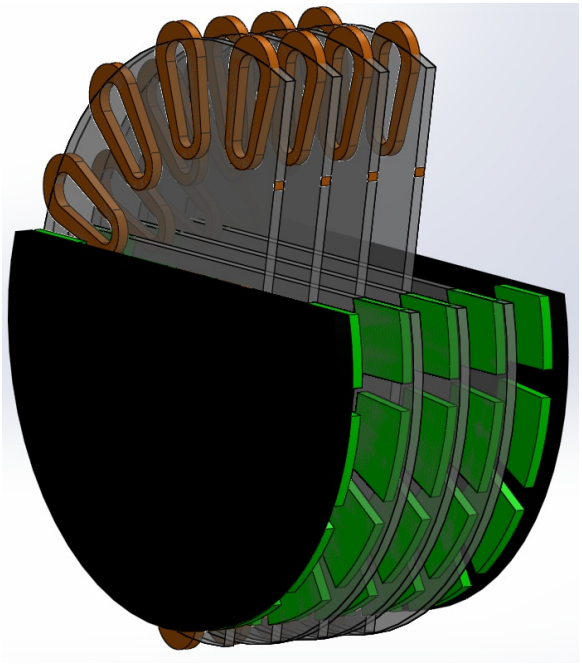

Fig. 3. Multi disc machine from [1]

In *the double sided* topology, a rotor disc is centered between two stator discs or a stator disc is centered between two rotor discs. These two topologies are referred to as either *double sided internal stator* topology or *double sided internal rotor* topology. The advantage of the internal rotor arrangement is improved heat removal from the current carrying stators because they are positioned at the end of the machine. This also eliminates the need for a separate housing.

An example of *the double sided internal rotor* topology is shown in Fig. 2. Like in the *single sided machine*, the magnets in the rotor disc alternate between the north and the south pole facing the stator. There is also a north to south correlation between the magnets in each rotor disc so that the flux goes from one magnet to the other before turning. One advantage of this topology is that the axial forces experienced in *the single sided machine* are cancelled out. It also allows an iron free design, since the flux is directed through the stator by magnets on each side. Heat removal from the internal, current carrying stator disc is less effective with this design than with *the external stator* approach.

Multi disc arrangements may be a solution when the diameter of the machine is constrained. By stacking more discs in series, higher torque can be obtained. Doing this will not increase the efficiency of the machine, because the arrangement is made up of several machines with the same efficiency. The losses will increase proportionally with the torque increase. The end coil volume for each stator disc will also remain the same. A simple *multi disc* arrangement is shown in Fig. 3.

IV. PREVIOUS WORK

An analysis of a novel coil design for axial flux machines has been performed in [1]. The investigation was based on a coil design patented by J.E. Brennvall [12] at Greenway Energy AS. The patent concerns a coil assembly for a three phase brushless PM axial flux multi disc machine. The coils have machined cuts, so that they can cross over each other and overlap like shown in Fig. 1. By overlapping the coils, the previously empty space within one coil will be filled with conductors from the adjacent coils. The result is an easily assembled, completely flat disc that allows a compact multi disc arrangement and a very high fill factor. A cooling medium flowing through the air-gap will have a large contact surface with the stator and provide excellent cooling capabilities. Higher current densities will be available with sufficient cooling.

During the investigation performed in [1], solid conductor single turn wave winding was chosen for further work because of the simplicity and easy assembly of the design. The solid conductor material was intended to be aluminium. These choices and other alternatives are presented further in the text.

A. Solid conductor versus wired conductor

Solid conductors have larger AC-losses than wired conductors because of the increased cross-section. The advantage of a solid conductor is an increased ability to transfer heat. Wired conductors must be insulated from each other to avoid short circuiting. Insulating materials have very poor heat transfer capabilities. To remove the heat generated in the center of a wired coil, the heat must be transferred from one wire to the next until it reaches the surface. For each coil the heat travel through, the poor heat transfer capability of the insulations must be overcome. It was shown in [1] that the insulation

will create a temperature difference between each conductor leading to much higher temperature in the center of the coil. For solid conductors the difference between the surface and the center was proven to be only $0.05\,^{\circ}\mathrm{C}$. This means that the temperature inside the conductor can be controlled by controlling the temperature on the surface. Cooling the surface efficiently will cause the center to be cooled as well.

Because the cooling capability is the main feature for this design, the solid conductor was chosen. Having solid conductors also increases the fill factor of the machine. Because of the previously mentioned AC-losses and the cooling ability, the design is best suited for low frequency, low speed machines with high torque density.

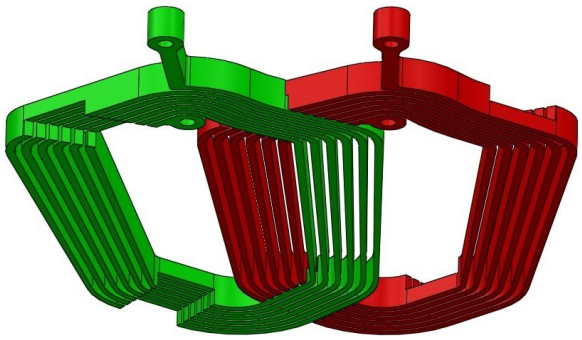

Fig. 4. Assembly of two lap-winded coils from [1]

B. Comparison of aluminium and copper as conductor material

Aluminium and copper was compared as conductor material for the design. Copper has excellent conductive abilities and is most commonly used as conductor in electric machines today [1]. Aluminium has only about 60% of coppers conductive ability, but has other attributes that makes it competitive. The price of copper has increased during the last decade, making it an expensive metal [16], [17]. Aluminium is a cheap metal and weighs considerably less. It also oxides instantly, giving the metal a resistive oxidation layer. This oxidation layer conducts heat well and provides a protecting surface. To increase the oxidation layer, the aluminium can be anodized. Copper however, oxides slowly and the oxidation layer is difficult to remove to create a good contact surface. The copper also has to be coated with an insulator with considerably lower heat transfer capability.

When using uninsulated copper, the cooling mediums dielectric strength must be suited for the voltage level. Aluminium is better suited when using water as a cooling medium, is cheaper and weighs less. Because of this, copper is more suited for high performance applications.

C. Stator Prototupe Manufacturing, Assembly and Testing

A stator prototype was manufactured and tested to investigate the practical challenges related to the design and to prove that the design can work in a three phase motor [1]. The prototype was financed by Greenway Energy AS and manufacture at Finmekanisk Verksted in Realfagsbygget at The Norwegian University of Science and Technology. The parameters of the prototype were chosen to fit the DNV Fuel Fighter motor, so that the same housing, shaft, rotor and test equipment could be used. The prototype can be seen in Fig. 2. The stator had a total of 48 poles and one turn per phase per pole. The magnets on the rotor were laid in a $45\,^{\circ}\mathrm{C}$ Halbach array. The air-gap magnetic field from the array was highly sinusoidal and had its peak at 1.05 T. The machine was iron free with an out diameter of 320 mm. The fill factor for single stator disc was calculated to be 91.9% [1]. A full study of the motor was performed by John Ola Buy in his master thesis at the Institute of Electric Power Engineering [18] He designed the high performance axial flux motor that was used in the Shell Eco Marathon race in 2013.

D. Manufacturing and assembly

One of the strengths of a wave-winding solid coil like the one in this design is that an entire winding can be manufactured as one piece. There are two versions of the windings, where one has its cuts on the same side while the other has alternating cuts. This is done to successfully assemble a stator layer and is shown in Fig 2. When the three phases are assembled, there are two windings with alternating cuts and one with cuts on one side. One of the windings with alternating cuts is turned upside down to fit in the cuts not occupied by the other.

The conductor was originally meant to be aluminium but no suitable alloy was found in time. Because of this, copper was chosen as the conductor material. A $1000 \times 2000 \times 4mm$ copper plate was cut into 10 wave windings using water cutting. A CNC miller was then used to make the machined cuts into the windings. A mold was made to hold the windings still during manufacturing and an aluminum ring was used to force the windings into the mold. Lastly, the connectors were separated by using a band saw after being left connected to provide better stability during manufacturing. Two layers electrical insulation tape laid in an X shape in the machined cuts were used as insulation between the phases. The cuts proved to be too narrow and the sharp edges left by the miller tore the tape. To fix this issue, the cuts were rubbed down using sand paper and new layers of tape were laid down.

When the insulation was done, each stator disc was assembled and cast in epoxy. Holes were then machined into the epoxy to fit the shaft, bolts and screws. The stator disc prototype was then ready for testing.

An even more detailed description of the process can be found in [1].

E. Laboratory testing

The finished stator prototype was tested using Shell Eco Marathon groups housing, shaft and equipment. The rotor assembly proved difficult, resulting in too little space for two stator discs. The testing was therefore only performed on one disc.

The test results were compared to a theoretical model for the machine. The phase resistance of the analytical model proved

reliable, but the torque and voltage constants were 30% too high. By reducing the air gap magnetic field in the analytical model by 30%, the voltage and torque constants converge. To not go into too much detail about the model and the test results, the reader is encouraged to read [1] for further detail. The table of efficiency results can however be seen in Table I. The maximum efficiency was measured to about 25% at 120 rpm, and 170A with air-cooling. Better efficiency and performance is expected with water cooling.

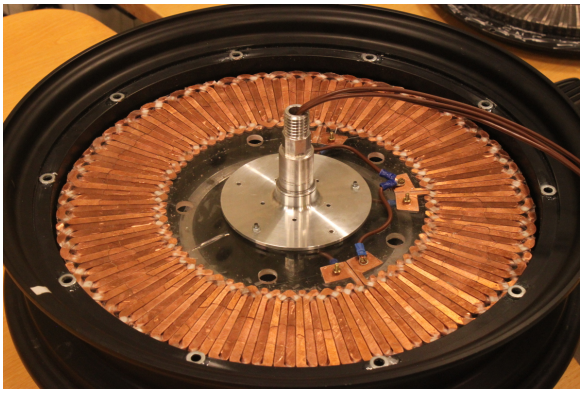

Fig. 5. Assembly of two lap-winded coils from [1]

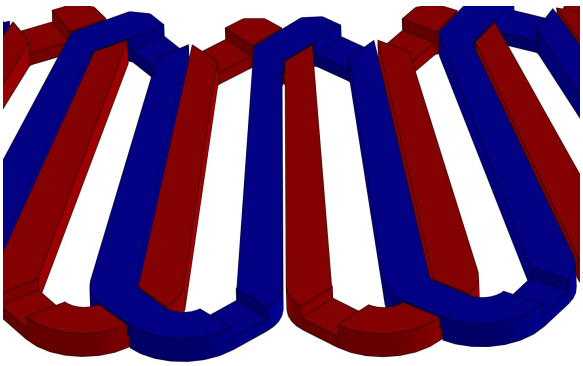

Fig. 6. Assembly of two lap-winded coils from [1]

TABLE I

EFFICIENCY MEASUREMENTS

Speed n [rpm]	Phase Current rms [a]	Efficiency (η, speed, current)
10	7	5.12 %
20	14.7	3.72 %
10	19.3	19.95 %
20	29	17.45 %
40	29	3.4 %

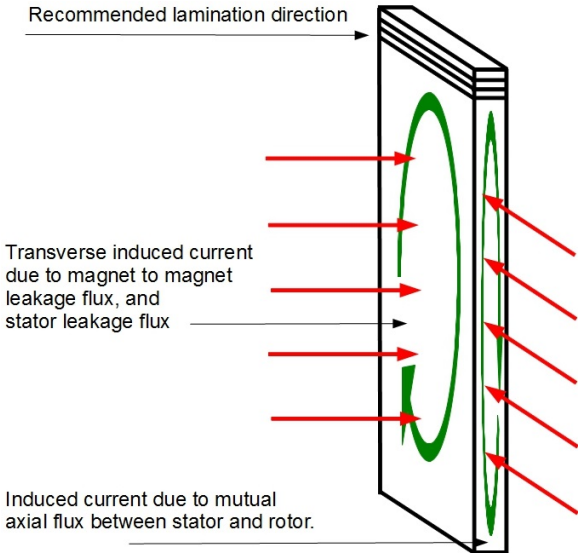

Fig. 7. Lamination of iron teeth from [1]

F. Laminated Iron in the Design

Laminated iron is introduced to the stator to strengthen the mechanical design of the motor, to focus the air-gap magnetic flux and increase the overall performance of the machine. The laminations lead the magnetic flux so that only the air-gap must be overcome instead of the air-gap and the axial depth of the stator. Because of this, less PM volume is required to produce a strong, sufficient magnetic flux density. Iron cores will lead to a cheaper machine that is better suited for industrial applications. The iron slots will reduce the fill factor by taking up space from the conductors, but will also allow longer axial depth. Wide conductors have very high eddy current losses and by reducing the conductor width the eddy current losses caused by magnetic flux will also be reduced.

Introducing an iron core leads to some complications as well as the positive effects previously mentioned. There will be cogging torque because of the changing reluctance seen by the magnets as they rotate. The iron must also be laminated to limit the eddy currents induced by the air-gap magnetic field. By using lamination, the core will become an equivalent to many small individual circuits. By dividing the core into many thinner bits, this will prevent most of the eddy currents in the core. The lamination can be produced by cutting rectangular formed, same sized lamination and stacking them together. The stack must be coated with insulation because of the non-insulated conductors. The magnetic field conducted by the lamination will only be in axial direction. Lamination is cheap and the production of it can easy be automated because each plate is identical. However, the assembly of the laminations in a stator with multiple discs with a given distance is complicated.

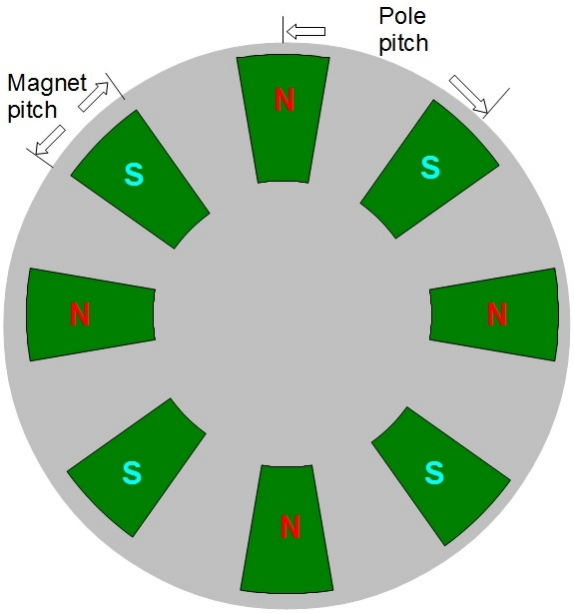

Fig. 8. simplified figure of rotor geometry [1]

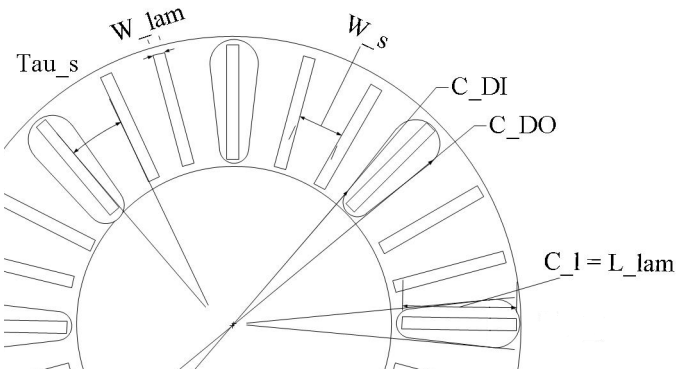

Fig. 9. Simplified figure of stator geometry

TABLE II

PARAMETERS IN FIG. 9

Tau_{-p}, τ_p	Pole pitch	[-]
Tau_s, τ_s	Slot pitch	[-]
C_{DO}	Outer diameter of coil active area	[mm]
C_{DI}	Inner diameter of coil active area	[mm]
L_{lam}	Lamination length (radial)	[mm]
C_l	Length of conductor active area (radial)	[mm]
W_{lam}	Lamination width	[mm]
w_s	slot width	[mm]

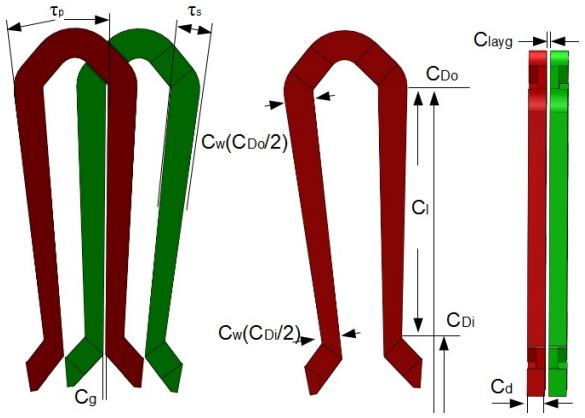

Fig. 10. Coil geometry and parameters from [1]

TABLE III

SET PARAMETERS

n	Rated rotational speed	30 [rpm]
E_{ph}	Rated RMS induced voltage ph-n	125 [V]
T_{req}	Required average torque	6250 [Nm]
q	Number of slots per phase per pole	[-]
N_{ph}	Number of phases	3 [-]
K_d	Ratio between outer and inner diameter	0.6[-]

V. MACHINE MODEL

A. Machine Specifications, Geometry and Variables

The machine optimized in this report is an axial flux permanent magnet machine made for low speed applications. The topology considered is a double sided internal stator with laminated iron. A simplified figure of rotor and stator geometry is shown in Fig. 8 and 9 respectively. The parameters in Fig. 9 and their dimensions are shown in Tab. II. A few key parameters describe the geometry and are used to calculate the dependant parameters. The number of slots per pole per phase, q, is kept equal to 1 to simplify the magnetic model and the calculation of the geometric dependant parameters. The coil geometry is based on the coils presented in [1] and can be seen in Fig. 10 together with the parameters used in the design. The coils are limited to a single turn wave winding topology and is made out of aluminium.

A number of parameters are fixed and work as the rated conditions of the machine. These set parameters are shown in Tab. III. Costs coefficients for the different materials can be seen in V. Other material properties, like conductivity, density and relative permeability is set in the machine model. The independent variables used to optimize the machine model can be seen in Tab. IV.

α_m is ratio between magnet pitch and pole pitch, and is chosen as a variable instead of magnet width. This is because the magnet width can't be physically bigger than what the pole pitch allows. Letting α_m vary instead of magnet width will prevent this from happening.

TABLE IV

INDEPENDENT VARIABLES

	Lower bound	Upper bound
Outer diameter of active coil, C_{outer}	0.2 m	1.0 m
Number of poles, N_p	20	60
Current density,J	3 A/mm^2	8 A/mm^2
Number of coil layers, N_{lay}	12	34
Depth of magnets (axial), M_d	5 mm	10 mm
Magnet width / pole pitch ($\frac{w_m}{\tau_p}$), α_m	0.2	0.99
Air gap length, g	1 mm	6 mm
Conductor depth, C_d	1 mm	4 mm

TABLE V

COST COEFFICIENTS

$C_{Aluminium}$	C_{pm}	$C_{laminations}$	C_steel
1.275 €/kg	85 €/kg	4 €/kg	6 €/kg

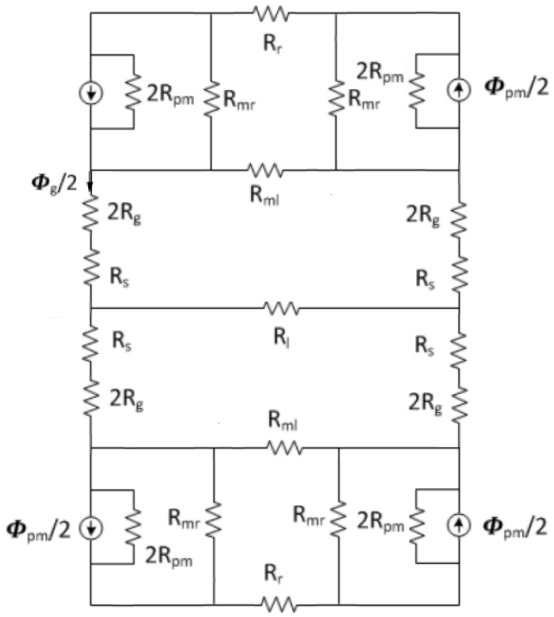

Fig. 11. Magnetic circuit model for air gap flux density calculation

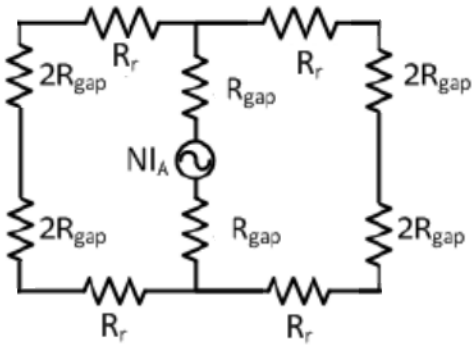

Fig. 12. Simplified section of armature reacton circuit for calculation of electric loading

B. Magnetic Model

The electromagnetic model used is based on magnetic circuits and is shown in Fig. 11. The magnetic circuit spans a whole pole pitch, $1/N_p$ of the machine, from the middle of one magnet to the middle of the next. This is the only section necessary to calculate the air gap flux from the permanent magnet. The model is limited to 2-D, calculated at average radius, assuming a constant magnetic and electric loading on its active length. A cross-section of a pole pitch at average radius can be seen in Fig. 13. Due to the 2-D limitations, AC-losses, total harmonic distortions, back-EMF waveforms and cogging are not included in this model. Cogging forces in an iron cored machine with number of slots per pole per phase equal to one are significant, and effort has been done by Greenway Energy to reduce these forces [41].

Because of the slotted stator, not nearly all of the flux lines from the rotor permanent magnet will be able to take the shortest path to the laminated iron. This leads to a phenomenon where air gap will seem to be longer than the physical distance. To make up for this, the air gap length is multiplied with Carter's coefficient, k_c. Carter's coefficient is calculated with the following equations:

$$k_c = [1 - \frac{2w_s}{\pi\tau_s}(arctan(\frac{w_s}{g} - \frac{g}{2w_s}ln(1 + \frac{w_s}{g})))]^{-1} \quad (12)$$

The magnetic circuit shown in Fig. 12 is used to find the electric loading for loaded condition. The torque produced is found with an equation derived from [1]:

$$T = C_d M B_g N_p N_{lay} q 2\sqrt{2} J \overline{C}_w cos(\frac{\pi}{6}) C_l r_{avg} \quad (13)$$

where C_d is the conductor depth in axial direction, M is the number of machines, B_g is the air gap flux density and N_{lay} is the number of coil layers. J is the current density, q is the number of slots per pole per phase, $\overline{C}_w$ is the average conductor width, C_l is the length of the active conductor area and r_{avg} is the average radius of the conductors.

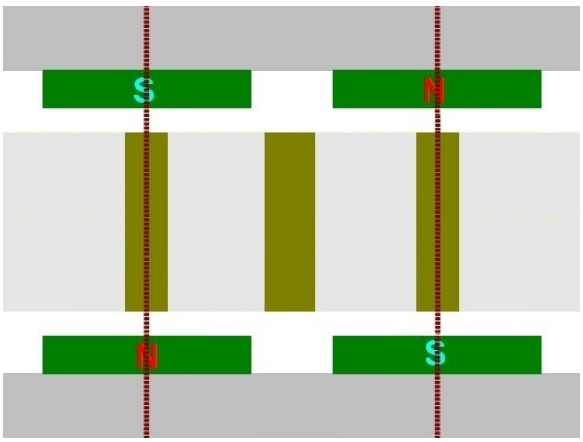

Fig. 13. Side view of the double sided internal stator topology from [1]

C. Objective function and restrictions

Reducing the cost of electrical machines is one of the main challenges when optimizing a machine. An objective function for optimizing the material cost of an axial flux permanent magnet machine can be formulated as:

$$C(X) = M_{backiron} * C_{steel} + M_{laminations} * C_{laminations} + M_{conductor} * C_{aluminium} + M_{PM} * C_{PM} \quad (14)$$

M is the mass of each material and C is the cost coefficients given in Tab. V.

Another optimization goal is the total lifetime cost:

$$Z(X) = C(X) + \sum_{i=1}^{k} \frac{E_{loss,yearly} * C_{energy}}{(1 + k_{discount})^k} \quad (15)$$

Where k is the lifetime of the machine in years, $k_{discount}$ is the discount rate, $E_{loss,yearly}$ is the yearly energy loss and C_{energy} is the energy price. The yearly energy consumptions were calculated with a very simplified calculations using full load equivalent hours. Only 10 yearly full load equivalent hours where used to find the lifetime energy cost, and these costs still outweighed the material cost significantly.

Constraints must be put in the model to guide the optimization in the wanted direction. The constraints given in this model was a minimum torque, T_{req}, a required back-EMF, E_req, a minimum lamination width, a minimum conductor width and a minimum ration between iron and air gap surface area. A restriction on power factor were also set later to improve the results. The minimum torque required in the model was 6250 Nm, and the minimum back-EMF was 125 V, while the minimum tooth width and conductor width were both 3mm.

TABLE VI

RESULT: UNOPTIMIZED

	Cost	2684 €
	Total weight	113 kg
	Independent variables:	
C_{outer}	Outer diameter of active coil	360 mm
N_p	Number of poles	40
J	Current density	10.3 A/mm^2
N_{lay}	Number of coil layers	21
M_d	Depth of magnets (axial)	6.667 mm
α_m, $(\frac{w_m}{\tau_p})$	Magnet width / pole pitch	0.8
g	Air gap length	1 mm
C_d	Conductor depth	1.5 mm
	Machine parameters:	
L	Total active length	361 mm
η	Efficiency	29.6 %
pf	Power factor	0.97
w_{alu}	Aluminium weight	22 kg
w_{pm}	Magnet weight	28 kg
w_{Fe}	Iron weight	45 kg
w_{Steel}	Steel weight	19 kg
M	Number of machines	5
$V_{T,LL}$	Terminal voltage, l-l	616 V

D. Model comparison

An analytical model made for quick calculations on an AFPM with laminated iron was presented [1]. The model made for this report were run with the same specifications as in [1] for comparison. The resulting machine design is given in VI. This design will be referred to as the original design later in this report. Note that the current density is larger than the upper boundary used when optimizing. This is because the machine was meant to be water cooled. However, the electric resistivity of oxidized aluminium proved to the too low for water cooling. The upper limit of the current density was therefore chosen to be 8 A/mm^2.

VI. GRAPHICAL USER INTERFACE

A graphical user interface (GUI) were made by using GUIDE, MATLAB's graphical user interface designer. The GUI was designed to do optimizations with hybrid optimizations and display results directly in the GUI. The user can define constraints on maximum diameter, length and line to line voltage, and minimum torque, power factor and efficiency directly in the UI. The program runs even without any constraints however, the unconstrained vary a lot more than the constrained. Constraints on minimum lamination and conductor width are static and can't be changed through the GUI. The objective function optimized can be changed through a drop-down menu. The objective functions available are total material weight, total material cost and total lifetime cost. Fig. 14 through 16 shows how the user interface is used. The results in Fig. 15 are found using total material cost as objective while the results in Fig. 16 are found with total lifetime cost.

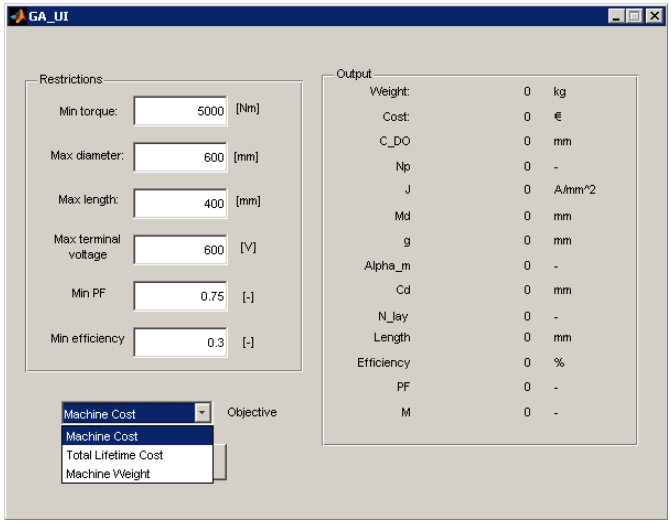

Fig. 14. Screen shot of the user interface showing the drop-down menu

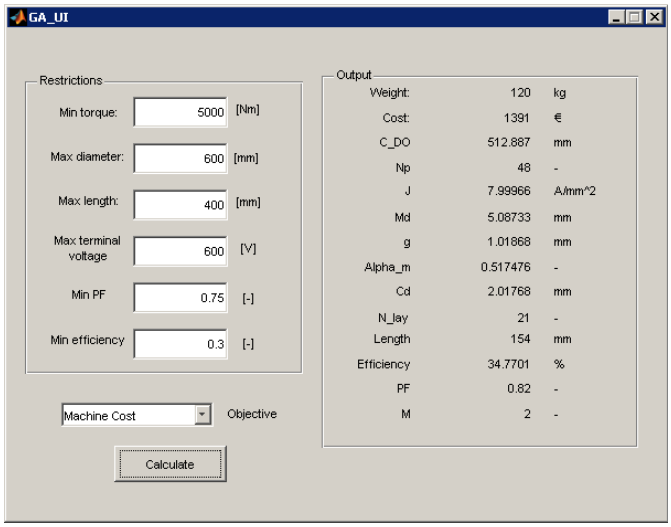

Fig. 15. Screen shot of the user interface showing optimizations done with total material cost as objective

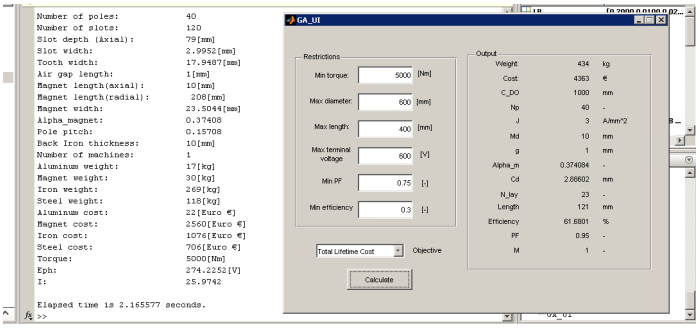

Fig. 16. Screen shot of the user interface showing optimizations done with total lifetime cost as objective

VII. RESULTS

Different optimization techniques were run to test how they performed. The optimization methods tested was Genetic Algorithm, Gradient Based Optimization with Interior-Point and a hybrid of Genetic Optimization and Interior-Point. Optimizations were first run without any restrictions to efficiency and power factor to see how cheap the machine could be made. Hybrid GA optimization was then run with restrictions to power factor to see how this would affect the design.

The machine model was first optimized with machine cost as the objective function. Both GA and hybrid GA were run with a population of 25 and 20 generations with a crossover fraction of 0.40. The average computation time of all the optimizations run was 4.27 s with 5.5 s as the highest value. Regular GA gave an average material cost of 1237.2 €, and 158.2 kg material weight. This is a 53.90 % reduction in cost in average and a 40 % weight increase compared to the unoptimized, static model. The designs found without any restrictions gave a very poor power factor and efficiency. The average efficiency found with regular GA was 13.92 % and the average power factor was 0.308.

Hybrid GA gave the he absolute cheapest design, which can be seen in table VII. The cost found by this optimization was 58.86% cheaper than the cost found in the original design. The optimized machine had an efficiency of only 13.7% and a power factor of 0.3. The total weight of the machine was 144 kg, which is 31 kg more than the unoptimized result. Hybrid GA were in average able to find a design cost 1217.8 € and a material weight of 148.4 kg. The average efficiency of the designs found was 17.96 % and the average power factor was 0.398. Total lifetime cost of the cheapest design was 1424346 €.

The initial design found with GA and hybrid GA, without constraints on power factor, chose 1 machine instead of a multi disc arrangement. The designs had a diameter that varied between 500 and 600 mm. The only active boundary in the cheapest design was the lower boundary on the air gap. Other than that, the current density and magnet depth was very close to the upper and lower bound respectively. The line to line terminal voltage, $V_{T,LL}$, found in these optimizations were all in the range of 1 kV.

TABLE VII

CHEAPEST DESIGN WITH UNRESTRICTED, HYBRID GA

	Cost	1104 €
	Total weight	144 kg
	Independent variables:	
C_{outer}	Outer diameter of active coil	559 mm
N_p	Number of poles	52
J	Current density	7.928 A/mm^2
N_{lay}	Number of coil layers	32
M_d	Depth of magnets (axial)	5.07 mm
α_m, $(\frac{w_m}{\tau_p})$	Magnet width / pole pitch	0.486
g	Air gap length	1.00 mm (LB)
C_d	Conductor depth	2.80 mm
	Machine parameters:	
L	Total active length	129 mm
η	Efficiency	13.7 %
pf	Power factor	0.3
w_{alu}	Aluminium weight	16 kg
w_{pm}	Magnet weight	6 kg
w_{Fe}	Iron weight	88 kg
w_{Steel}	Steel weight	32 kg
M	Number of machines	1
$V_{T,LL}$	Terminal voltage, l-l	1230 V

TABLE VIII

RESULT FROM GRADIENT BASED OPTIMIZATION

	Cost	1585 €
	Total weight	166 kg
	Independent variables:	
C_{outer}	Outer diameter of active coil	328 mm
N_p	Number of poles	40
J	Current density	8 (UB) A/mm^2
N_{lay}	Number of coil layers	23
M_d	Depth of magnets (axial)	5 mm (LB)
α_m, $(\frac{w_m}{\tau_p})$	Magnet width / pole pitch	0.5467
g	Air gap length	1 (LB) mm
C_d	Conductor depth	3.135 mm
	Machine parameters:	
L	Total active length	536 mm
η	Efficiency	28.6 %
pf	Power factor	0.88
w_{alu}	Aluminium weight	29 kg
w_{pm}	Magnet weight	12 kg
w_{Fe}	Iron weight	106 kg
w_{Steel}	Steel weight	20 kg
M	Number of machines	5
$V_{T,LL}$	Terminal voltage, l-l	552 V

The optimizations done with the Gradient Based Interior-Point algorithm gave a lot less variance than the other two optimization techniques gave. Every time it was run it gave a machine cost of 1585 €. The weight of the optimized machine was 166 kg with an efficiency of 28.8 % and a power factor of 0.88. Instead of having only one machine, the optimization chose to put 5 double sided internal disc machines together in a multi disc arrangement. The diameter of the machine was 328 mm with an active length of 536. Lower air gap length, upper current density and magnet depth was the limiting variables in this design also.

A. Hybrid GA with restrictions to power factor

Restrictions were put on the power factor to make the optimization results more applicable for actual electrical machines. The power factor were first restricted to 0.5, then 0.75 and lastly to 0.85. The cheapest designs found with these restrictions are shown in Tab. IX , Tab. X and Tab. XI respectively. Even with a power factor of 0.85, the cost of the machine was reduced to 1537 €.

TABLE IX

RESULT FROM HYBRID GA WITH PF ≥ 0.5

	Cost	1190€
	Total weight	130 kg
	Independent variables:	
C_{outer}	Outer diameter of active coil	430 mm
N_p	Number of poles	48
J	Current density	7.99 (UB) A/mm^2
N_{lay}	Number of coil layers	23
M_d	Depth of magnets (axial)	5.00 mm (LB)
α_m, $(\frac{w_m}{\tau_p})$	Magnet width / pole pitch	0.563
g	Air gap length	1.001 (LB) mm
C_d	Conductor depth	2.757 mm
	Machine parameters:	
L	Total active length	229 mm
η	Efficiency	21.5 %
pf	Power factor	0.55
w_{alu}	Aluminium weight	21 kg
w_{pm}	Magnet weight	8 kg
w_{Fe}	Iron weight	77 kg
w_{Steel}	Steel weight	24 kg
M	Number of machines	2
$V_{T,LL}$	Terminal voltage, l-l	739 V

TABLE X

RESULT FROM HYBRID GA WITH PF ≥ 0.75

	Cost	1490 €
	Total weight	139 kg
	Independent variables:	
C_{outer}	Outer diameter of active coil	516 mm
N_p	Number of poles	46
J	Current density	8 (UB) A/mm^2
N_{lay}	Number of coil layers	34 (UB)
M_d	Depth of magnets (axial)	5 mm (LB)
α_m, $(\frac{w_m}{\tau_p})$	Magnet width / pole pitch	0.53643
g	Air gap length	1 (LB) mm
C_d	Conductor depth	1.4156 mm
	Machine parameters:	
L	Total active length	177 mm
η	Efficiency	37.1 %
pf	Power factor	0.75
w_{alu}	Aluminium weight	18 kg
w_{pm}	Magnet weight	11 kg
w_{Fe}	Iron weight	84 kg
w_{Steel}	Steel weight	26 kg
M	Number of machines	2
$V_{T,LL}$	Terminal voltage, l-l	836 V

TABLE XI

RESULT FROM HYBRID GA WITH PF ≥ 0.85

	Cost	1537 €
	Total weight	142 kg
	Independent variables:	
C_{outer}	Outer diameter of active coil	436 mm
N_p	Number of poles	46
J	Current density	8 (UB) A/mm^2
N_{lay}	Number of coil layers	25 (UB)
M_d	Depth of magnets (axial)	5 mm (LB)
α_m, $(\frac{w_m}{\tau_p})$	Magnet width / pole pitch	0.5475
g	Air gap length	1 (LB) mm
C_d	Conductor depth	2.0533 mm
	Machine parameters:	
L	Total active length	262 mm
η	Efficiency	33.3 %
pf	Power factor	0.85
w_{alu}	Aluminium weight	21 kg
w_{pm}	Magnet weight	13 kg
w_{Fe}	Iron weight	86 kg
w_{Steel}	Steel weight	22 kg
M	Number of machines	3
$V_{T,LL}$	Terminal voltage, l-l	629 V

B. Using a different objective function

When running with total lifetime cost as the objective function, the machine design changes completely. A table of the results from an optimization run with this objective function is shown in Tab. XII. The material cost of the design found was 4742 €, while the total lifetime found was 289,851 €. The machine design was limited by different boundaries with this objective function than . Air gap length was the only variable kept at the same value. The efficiency of the machine increased to 58.5 %, and the power factor was 0.9. The material weight of the machine increase to 4.76 times the weight of the original design.

TABLE XII

RESULT FROM HYBRID GA WITH TOTAL COST AS OBJECTIVE FUNCTION

	Cost	4742 €
	Total weight	538 kg
	Independent variables:	
C_{outer}	Outer diameter of active coil	1000 (UB) mm
N_p	Number of poles	40
J	Current density	3(LB) A/mm^2
N_{lay}	Number of coil layers	23
M_d	Depth of magnets (axial)	10 mm (UB)
α_m, $(\frac{w_m}{\tau_p})$	Magnet width / pole pitch	0.367
g	Air gap length	1.001 (LB) mm
C_d	Conductor depth	4 (UB) mm
	Machine parameters:	
L	Total active length	147 mm
η	Efficiency	58.5 %
pf	Power factor	0.9
w_{alu}	Aluminium weight	21 kg
w_{pm}	Magnet weight	30 kg
w_{Fe}	Iron weight	362 kg
w_{Steel}	Steel weight	125 kg
M	Number of machines	1
$V_{T,LL}$	Terminal voltage, l-l	600 V

VIII. DISCUSSION

Hybrid GA were able to get the lowest cost of the machine, but were only able to find designs that were 19.4 € cheaper in average than regular GA. The best design found was 58.86 % cheaper than the original design, but weighed 31 kg more. It is obvious from that result that lower weight doesn't necessarily give a cheaper machine. Optimizing a machine with regards to weight may not give the cheapest solution. This is because different materials have different costs. The most expensive material in the model is by far the permanent magnets, with a cost of 85 € pr kg. The cheapest design found by hybrid GA was in fact the design with the lowest permanent magnet weight. Increasing the weight of other materials to reduce the permanent magnet volume may prove beneficial. The axial depth of the permanent magnet were kept at its lower bound in every single optimization design with the total lifetime optimization as the only exception. If not for the lower boundary of magnet depth, the optimization algorithm would've chosen to make the magnet too thin. The magnet width varied through the ratio between magnet pitch and pole pitch, α_m, but wasn't optimized to become the lower boundary despite the high material cost. This is because a certain magnet width had to be retained to get a sufficient air gap flux density.

The cheapest design found with hybrid GA had an efficiency of only 13.7 % and a power factor of 0.3. The material cost was almost 60 % lower than the original cost, but the low efficiency and power factor makes the design inapplicable. Constraints must be applied to keep the result

within reasonable values. With a power factor restricted to minimum 0.85, hybrid GA were able to find an optimized result with a material cost of 1573 € and an efficiency of 33.3 %. This designs efficiency is 3.7 % better than the original, and the material cost is 41.39 % less. This makes the constrained design a very good result.

The optimization result found by Gradient Based Interior-point optimization was 1099 € cheaper than the original design but still 481 € more expensive than the design found by hybrid GA. The same result were found every time with no deviation at all. This indicates that the Gradient Based optimization failed to escape a local optima. The solution had an efficiency of 28.8% and a power factor of 0.88, which is comparable with the original design. Despite the similarity in power factor and efficiency, the optimized design had a material cost 40.94 % lower than the original. Even though the result found was a good design, the inability to escape local minima makes GA and hybrid GA better optimization techniques.

The current density were kept at the lower boundary through all the optimization except the total lifetime cost optimization. That is because no cost was associated with the current in the machine until the cost of energy was introduced in the lifetime cost optimization. There was no reason to decrease the current density before this objective function was used. By introducing a thermal model to the machine model, the head dissipation capability of the machine will limit the allowable current density.

The material cost found when optimizing the lifetime cost of the machine was 4.3 times greater than the lowest material cost found when optimizing material cost. This is because the lifetime cost of energy substantially outweighs the material cost, even when the amount full load hours were very low. The total lifetime energy cost found with only 10 full load hours were 1,424,346 € for the design with the lowest material cost, while the total lifetime energy cost 289,851 € for the design optimized with regards to total lifetime cost. The efficiency of the latter was 58.5 %. The efficiency of the machine would also be improved if copper were used as conductor material instead of aluminium. The material cost of the machine would however increase with copper conductors.

The computation time of hybrid GA were 4.27 seconds in average. This run time is far too low to justify the use of parallel processing for the amount of individuals and generations used in this report. There is also no need to decrease the number of individuals and generations with a 5.5 second maximum computation time.

IX. CONCLUSION

An analytical model of the axial flux permanent magnet machine presented in [1] has been made. The model has been described and presented. Optimization of the model has been done with Genetic Algorithm, Gradient Based Interior-Point optimization and a hybrid combination of the two, hybrid GA. The optimizations were done with regards to either material cost or total lifetime cost.

Gradient based Interior-Point optimization failed to escape local optima and were hence unable to find the global minima. It were however able to find the best solution within area of the local optima. GA and hybrid GA were able to find the region of the global optima, but had problems converging on the optimal point. The best solution to material cost optimization was found by hybrid GA. The material cost of this design was 58.86% cheaper than the original, but had too low efficiency and power factor to be applicable.

Constraints were put on power factor to improve the feasibility of the optimizations. With restrictions on the power factor, a design with 40.94 % improved material cost, 33.3 % efficiency and a power factor of 0.85 was found. With restrictions on diameter, length, voltage and efficiency, a machine can be optimized to fit almost any application.

When optimizing with total lifetime cost as objective function, the material cost was increased to 4.3 times the lowest solution found with material cost as objective function. The lifetime energy cost were decreased with 82.58 % compared to the design with lowest material cost.

Parallel processing was deemed unnecessary because of the short computation time and the simplicity of the model. Even with a moderately simple model can a machine design be drastically improved with a computational optimization techniques like Genetic Algorithms and Gradient Based Optimization.

X. FUTURE WORK

A natural extension to the work presented in this report would be to include a thermal model in the machine model. It is also of interest to include a function for eddy current loss calculations for stator laminations and rotor back iron.

The effect of broken windings in an AFPM of this design should be investigated. Broken windings may improve the cogging torque and harmonics of the machine.

ACKNOWLEDGEMENT

I would like to thank my supervisors, Robert Nilsen at the Norwegian University of Science and Technology and Jon Eirik Brennvall at Greenway Energy AS for providing me with guidance, structure and a goal to work towards. I would also like to thank Sigbjrn Lomheim for laying a solid foundation for my work and for giving me tips and aid. Zhaoqiang Zhang provided me assistance and guidance, for which I am very grateful.

Last but not least, I would like to thank my friends at the office who have brightened the early mornings and the late evenings. Erlend Engevik deserves special thanks for helping me with GA and LaTeX, even on his vacation on Rhodos.

REFERENCES

[1] S. Lomheim, *Analysis of a Novel Coil Design for Axial Flux Machines*, Master Thesis, NTNU, Norway, 2013, Department of Electric Power Engineering.

[2] J.F. Gieras, R. Wang, M. J. Kamper, *Axial Flux Permanent Magnet Brushless Machines*, Second Edition.

[3] D. C. Hanselmann *Brushless Permanent Magnet Motor Design*, McGraw-Hill, Inc, New York, 1994.

[4] Capponi F.G, Caricchi F., De Donato G., *Recent Advances in Axial Flux Permanent-magnet Machine Technology*, IEEE Transaction on Industry Applications, VOL. 48, NO. 6, November/December 2012, Page(s): 2190 2205.

[5] Caricchi, F., Capponi, F.G., Crescimbini, F., Solero, L., *Experimental study on reducing cogging torque and core power loss in axial-flux permanent-magnet machines with slotted winding,* Industry Applications Conference, 2002. 37th IAS Annual Meeting. Conference Record of the, vol.2, no., pp.1295-1302 vol.2, 13-18 Oct. 2002

[6] A. Parviainen, J. Pyrhnen, M. Niemel, *Axial Flux Interior Permanent Magnet Synchrounous Motor With Sinusodially Shaped Magnets*, 10th Internatonal Symposium on Electromagnetic Fields in Electrical Engineering, Poland, September 2001.

[7] D.J. Patterson, C W Brice, R A Dougal, D Kovuri *The "Goodness" of Small Contemporary Permanent Magnet Electric Machines*, Proceecings of the 2003 IEEE International Electric Machines and Dries Conference , IEMDC '03 Madison, Wisconsin, June 2003.

[8] F. Caricchi, F. Crescimbi, O. Honorati, G. Bianco, E. Santini, *Performance of coreless-winding axial-flux permanent-magnet Generator With Power Output at 400 Hz, 300 r/min* IEEE transactions on industry applications, vol. 34 NO. 6 November/December 1998.

[9] Price development of neodymium magnets, http://www.supermagnete.de/eng/faq/price, Visited 26.06.2014.

[10] Changes and trends for neodymium magnets. http://www.supermagnete.de/eng/faq/price Visited 20.11.2013

[11] J.F. Gieras, I.A. Gieras *Performance Analysis of a Coreless Permanent Magnet Brushless Motor*

[12] Patent on axial flux coil design, inventor: J.E. Brennvall, Applicant: Greenway Energy AS, J.E. Brennvall. Number: WO2012128646 at www.epo.org

[13] Anyuan Chen, Robert Nilssen, Arne Nysveen, *Harmonic Analysis and Comparison of the Back EMFs of Four Permanent Magnet Machines with Different Winding Arrangements*, Electrical Machines and Systems, 2008. ICEMS 2008. International Conference on , vol., no., pp.3043-3048, 17-20 Oct. 2008

[14] C. Studer, A. Keyhani, T. Sebastian, S.K. Murthy, *Study of cogging torque in permanent magnet machines* Industry Applications Conference, 1997. Thirty-Second IAS Annual Meeting, IAS '97., Conference Record of the 1997 IEEE , vol.1, no., pp.42-49 vol.1, 5-9 Oct 1997.

[15] Material properties of Aluminum: http://no.wikipedia.org/wiki/Aluminium Visited 26.08.2014

[16] Copper price variation: http://www.indexmundi.com/commodities/?commodity=copper Visited 26.06.2014

[17] Aluminum price variation: http://www.indexmundi.com/commodities/?commodity=aluminum Visited 26.06.2014

[18] John Ola Bu y, *Development of High Efficiency Axial Flux motor for Shell Eco-Marathon*, Master Thesis, NTNU, Norway 2013 Department of Electric Power Engineering

[19] F. Cariacchi, F. Crescimbini, O. Honorati, *Low-Cost Compact Permanent Magnet Machine for Adustable-Speed Pump Application*, IEEE Transaction on Industry Applications, Vol 34, No. 1 January/February 1998, pp 109-116.

[20] Z.Q. Zhu, D. Howe *Analytical Prediction of the Cogging Torque in Radial-field Permanent Magnet Brushless Motors*, IEEE Transaction on Magnetics, Vol. 28, No. 2, March 1992, pp 1371-1374.

[21] G.W. Cho, S. H. Woo, S. H. Ji, *Optimization of rotor shape for constant torque characteristic of IPM Motor*, International Conference on Electrical Machines and Systems (ICEMS) 2011, p. 1-4.

[22] X. Yang, D. Patterson, J. Hudgins, *Core Loss Measurement in a Fabricated Stator of a Single-sided Axial Flux Permanent Magnet Machine*, IEEE International Electric Machines and Drives Conference (IEMDC) 2013, p. 612-617.

[23] A. Ahfock and A.J. Hewitt, *Curvature-related eddy-current losses in laminated axial flux machine cores*

[24] J.R. Bumby, R. Martin, M.A Mueller, E. Spooner, N.L. Brown and B.J. Chalmers, *Electromagnetic design of axial-flux permanent magnet machines*

[25] A. Parviainen, *Design of Axial-Flix Permanent-Magnet Low-Speed Machines and Performance Comparison Between Radial-Flux and Axial-Flux Machines*, Thesis for Doctor of Science Degree, 19.04.2005.

[26] L. Chen, S. Sudo, Y. Gao, H. Dozono, K. Marumatsu, *Homogenization Technique of Laminated Core Taking Accout of Eddy Currents Under Rotational Flux Without Edge Effect*, IEEE Transaction on Magnetics, Vol. 49, No. 5, May, 2013, p. 1969-1972.

[27] R. Qu, M. Aydin, T.A Lipo, *Performance Comparison of Dual-Rotor Radial-Flux and Axial flux Permanent Magnet BLDC Machines*

[28] A. Parvianen, M. Niemel, J. Pyhnen, *Modeling of Axial FLux PM Machines.*

[29] E. L. Engevik, *Optimal Design of Tidal Power Generator Using Stochastic Optimization Techniques*, Master Thesis, NTNU, Norway, 2014, Department of Electric Power Engineering.

[30] A. Rkke *Gradient Based Optimization of Permanent Magnet Generator Design*, Department of Electrical Engineering, Norwegian University of Science and Technology, NTNU, 2014.

[31] J. Pyrhnen, T. Jokinen, V. Hrabovcova *Design of Rotating Electrical Machines*, John Wiley and Sons, Ltd, 2008

[32] A. Egea, G. Almandoz, J. Poza, G. Ugalde, A. J. Escalada *Axial-Flux-Machine Modeling with the Combination of FEM-2D and Analytical Tools*, IEEE TRANSACTIONS ON INDUSTRY APPLICATIONS, VOL. 48, NO. 4, JULY/AUGUST 2012 p. 1318 - 1326

[33] K. Abbaszadeh, S. S. Maroufian *Axial Flux Permanent Magnet Motor Modeling using Magnetic Equivalent Circuit*, K.N. Toosi University of Technology

[34] H. Tiegna, A. Bellara, Y. Amara, G. Barakat *Analytical Modeling of Open-Circuit Magnetic Field in Axial Flux Permanent-Magnet Machines with Semi-Closed Slots*, IEEE TRANSACTIONS ON MAGNETICS, VOL. 48, NO. 3, MARCH 2012, p. 1212-1226.

[35] A. Parviainen, M. Niemel, J. Purhnen, *Modeling of Axial Flux PM Machines*, Lappeenranta University of Technology, Department of Electrical Engineering.

[36] A. Bellara, H. Tiegna, Y. Amara, G. Barakat, *On Load Analytical Modelling of the Magnetic Field for Axial Flux Surface-Inset Permanent Magnet Machines with Semi-Closed Slots.*

[37] R. B. Mignot, F. Dubas, C. Espanet, C. Cuchet, D. Chamagne, *Original Design of Axial Flux PM Motor and Modeling of the Magnetic Leakage Using a Magnetic Equivalent Circuit*, 2012 IEEE Vehicle Power and Propulsion Conference, Oct. 9-12, 2012, Seoul, Korea

[38] H. Tiegna, Y. Amara, G. Barakat, *A New Quasi-3-D Analytical Model of Axial Flux Permanent Magnet Machines*, IEEE TRANSACTIONS ON MAGNETICS, VOL. 50, NO. 2, FEBRUARY 2014

[39] MathWorks. (2013) MATLAB — Global Optimization Toolbox — Users Guide — R2013b. $http://www.mathworks.com/help/pdf_doc/gads/gadstb.pdf.MathWorks.[Onlin$ $http://www.mathworks.com/help/pdf_doc/gads/gads_tb.pdf$

[40] Z. Michalewicz, Genetic Algorithms + Data Structures = Evolution Programs, 3rd ed. Springer-Verlag, 1996.

[41] Z. Zhang, J.E. Brennvall, R. Nilssen *Torque Ripple Reduction in an Axial-flux Jigsaw-coil Permanent Magnet Machine*

APPENDIX A
SETUP OF THE OPTIMIZATION ALGORITHMS IN MATLAB

A. Setup for Genetic Algorithms

```
% Genetic Optimization Algorithm using the built-in
% function ga in MATLAB

options = gaoptimset('FitnessScalingFcn',{
@fitscalingrank }, ...
'PopInitRange',[LB ; UB],...% Decides the range
of variables for the initial population
'StallGenL',10,...
'Generations',30, ... %Sets the number of
generations
'PopulationSize',25,...% Sets the population
size
'EliteCount',2, ... %Number of individes that
goes directly to next generation with out
crossover and mutation
'CrossoverFraction',0.4,... % Sets the
percentage of next generation that is
created by crossover, e.g. 40%
'UseParallel','always',... %Enables parallel
computing
'MigrationInterval',10,...
'MigrationFraction',0.1,...
'MigrationDirection','both', ...
'PopulationType','doubleVector',...
'SelectionFcn', { @selectiontournament [] });
... %Selects the selection function



[X fval exitflag output population scores] = ga (
@AnalyticTool_fun, 8, [], [], [], [], LB, UB,
@AnalyticTool_con, options);

%Setup for use of function ga for integer variables
intcons = [3,5]; % Variable 3 and 5 are integers

[X fval exitflag output population scores] = ga(
@objective_fun,nVar,[],[],[],[],LB,UB,
@constraint_fun,intcons,options);

%SelectionFcn must be removed from options, and
% intcons must be included before running ga(...)
```

B. Setup for Hybrid Genetic Optimization with Interior-point

```
%Setup of hybrid GA with built-in functions in
    Matlab
% Does not work with integer variables

hybridopts = optimset('Algorithm','interior-point','
MaxFunEvals',1500,'TolCon',1e-10,'TolX',1e-12,'
ObjectiveLimit',0); % run interior-point
algorithm
%Options for gradient based optimization,
% interior-point algorithm

options = gaoptimset('FitnessScalingFcn',
{@fitscalingrank }, 'popInitRange', [LB ; UB],
'stallGenL', 10, 'Generations', 20, 'PopulationSize'
    ,
25, 'EliteCount', 2, 'CrossoverFraction', 0.4,
'UseParallel', 'always', 'MigrationFraction', 10,
'MigrationFraction', 0.1, 'MigrationDirection',
'both', 'PopulationType', 'doubleVector',
'SelectionFcn', { @selectiontournament [] },
'HybridFcn', {@fmincon,hybridopts});
%GA options with hybridopts to make the hybrid

[X fval exitflag output population scores] = ga (
@AnalyticTool_fun, 8, [], [], [], [],
LB, UB, @AnalyticTool_con, options);
%Running hybrid
```

C. Setup for Gradient Based Optimization with Interior-point

```
%Setup for Gradient based optimization
% Interior-point with built-in functions
% in MATLAB

options = optimset('Algorithm','interior-point','
MaxFunEvals',1500,'TolCon',1e-10,'TolX',1e-12,'
ObjectiveLimit',0);

% run interior-point algorithm
[X fval exitflag output] = fmincon(
@AnalyticTool_fun, x_0, [], [], [],
[], LB, UB, @AnalyticTool_con, options);
```

APPENDIX B
MACHINE MODEL

```
function [f c ceq motor]=AnalyticTool(varb)

clc
clear motor

motor = struct('error',0);              %Declaring
    ms as a struct

%% Variable parameters %%

motor.variables.C_DO = varb(1);                  %
    Outer conductor diamter (active material) [m]
motor.variables.C_d = varb(2)/10;                %
    Conductor depth [m]
motor.variables.Np = varb(3)*1000;
                      % Number of poles
motor.variables.J = varb(4);                     %
    [A/mm^2] Current density / del av el ??
motor.variables.N_lay = varb(5)*1000;
                    % Number of coil layers
motor.variables.alpha_m = varb(6);               %
    Ratio between magnet width/pitch and pole pitch
motor.variables.g = varb(7)/10;                  %
    Air gap length [m]
motor.variables.M_d = varb(8)/10;                %
    Magnet depth. [m]

motor.variables.Np= round(motor.variables.Np);
motor.variables.N_lay = round(motor.variables.N_lay)
    ;

%% Constants %%

motor.constant.my_0 = 4*pi*1e-7;        % Relative
    permeability of vacuume
motor.constant.my_iron = 5000;          % Relative
    permeability of iron
motor.constant.my_pm = 1.05;            % Relative
    permeability of permanent magnet
motor.constant.my_air = 1;              % Relative
    permeability of air
motor.constant.sigma_alu = 35e6;        % [S/m]
    Conductivity of aluminium at 20 degrees (26
    .06.2014 http://en.wikipedia.org/wiki/
    Electrical_resistivity_and_conductivity)
motor.constant.sigma_steel = 10.4e6;    % [S/m]
    Conductivity of steel
motor.constant.sigma_air = 0;           % [S/m]
    Conductivity of air
motor.constant.rho_alu = 2700;          % Density of
     aluminium (26.06.2014 http://en.wikipedia.org/
    wiki/Aluminium) [kg/m^3]
motor.constant.rho_pm = 7700;           % Density of
     permanent magnet[kg/m^3]
motor.constant.rho_steel = 7870;        % Density of
     steel [km/m^3]
motor.constant.rho_lamination = 7870;   % Density of
     stator steel [kg/m^3]
motor.constant.lifetime = 20;           % Estimated
    lifetime of a motor

                                  %% Costs %% (ref
                                       needed for
                                      everything)

 motor.cost.C_laminations = 4;          % Euro pr.
     kilo material. Based on (Ref needed. Astrid)
 motor.cost.C_pm = 85;                  % Euro pr.
     kilo material. (ref needed)
 motor.cost.C_aluconductor = 1274.78/1000;         %
     Euro pr. kilo material. (26.06.2014: http://
    www.indexmundi.com/commodities/?commodity=
    aluminum&months=120&currency=eur)
 motor.cost.C_steel = 6;                % Euro pr.
     kilo material. (ref needed)
 motor.cost.disc_rate = 0.2;            % Discount
     rate.
 motor.cost.E_price = 0.24;             % Energy
     price [Euro/kWh].

                                  %% Set Parameters %%

motor.el.Eph_req = 125;                 % Min back
    emf [V]
motor.el.V_t_Req = 320;                 % Required
    line to line voltage  [V]
motor.mech.T_req = 6250;                % Required
    mechanical power [Nm] P_req
motor.mech.n = 30;                      % Mechanical
     rotational speed [rpm]
motor.mag.Br = 1.3;                     % Magnetic
    remenance flux density [T]
motor.el.N_ph = 3;                      % Number of
    phases
motor.geom.q = 1;                       % Slots pr.
    phase pr. pole
motor.geom.C_layg = 0.5/1000;           % Gap
    between cunductor layers. = d_wedge?
motor.geom.L_ed = 1/1000;               % [m]
    Lamination ekstra depth (
motor.geom.k_D= 0.6;                    % Ratio
    between out and inner diameter
motor.mech.Shaft_d = 20e-3;             % Shaft
    thickness [m]
motor.mech.time_fullP = 10;             % Hours
    yearly with full power consumption

                                  %% Limitations %%

lim_f = 30;                             % Maximum allowable
    frequency [Hz]
lim_tooth = 3e-3;                       % Minimum allowable
    tooth width [m]
Lim_PF = 0.5;                           % Minimum power
    factor.
Lim_Riron = 0.9;                        % Max ratio between
    iron and air gap surface area

%% Dependent parameters %%

motor.geom.c_totd = motor.variables.N_lay*(
    motor.variables.C_d+motor.geom.C_layg)-
    motor.geom.C_layg; % Stator active axial depth
motor.geom.L_alength = motor.geom.c_totd+(2*
    motor.geom.L_ed);                            %
    lamination axial length [m]
motor.geom.Ns = motor.geom.q*motor.el.N_ph*
    motor.variables.Np;                           %
    Number of slots
motor.el.f = motor.variables.Np*motor.mech.n/(60*2);
                                        % Electrical
     frequency
motor.mech.omega_m = motor.mech.n*2*pi/60;
                                                  %
    Mechanical speed [rad/s]
motor.el.omega_e = 2*pi*motor.el.f;

    % Electrical speed [rad/s]

motor.geom.tau_p = 2*pi/motor.variables.Np;
                                                 %
    Pole pitch [rad]
motor.geom.tau_s = 2*pi/motor.geom.Ns;

    % Slot pitch [rad] eller Ts = Tp/(ph*q)
motor.geom.tau_m = motor.geom.tau_p*
    motor.variables.alpha_m;
                                % Magnet pitch (am ->
     ratio between magnet pitch and pole pitch)
```

```
motor.geom.C_DI = motor.variables.C_DO*
    motor.geom.k_D;
                                    % Inner
    diameter of active coil
motor.geom.C_l = (motor.variables.C_DO-
    motor.geom.C_DI)/2;
                                % Conductor length
    (straigth area) =/ magnet length or slot radial
    length

motor.geom.r_O = motor.variables.C_DO/2;
                                                    %
     Outer radius of active material (med house
    diamter?)
motor.geom.r_I = motor.geom.C_DI/2;

    % Inner radius of active material ndvendig?
motor.geom.r_avg = (motor.variables.C_DO+
    motor.geom.C_DI)/4;                             %
     Average radius

motor.geom.L_lam = motor.geom.C_l;

    % slot depth (Radial length)
motor.geom.M_DO = motor.variables.C_DO*1.01;
                                                    %
    Magnet outer diameter
motor.geom.M_DI = motor.geom.C_DI*0.99;

    % Magnet inner diameter
motor.geom.M_l = (motor.geom.M_DO-motor.geom.M_DI)
    /2;                                     % Magnet
    length
motor.geom.M_w = motor.geom.tau_m*motor.geom.r_avg;
                                        % Average
    magnet width
motor.geom.R_iron = (motor.geom.tau_s*motor.geom.C_l
    )/(motor.geom.tau_m*motor.geom.M_l);% Ration
    between iron and air gap surface area
motor.geom.w_lam = 2*motor.geom.r_avg*tan(
    motor.geom.tau_s/2)*(motor.geom.R_iron);      %
    Lamination width
motor.geom.BI_D = motor.variables.M_d;

    % Back Iron axial depth
motor.geom.C_g = motor.geom.w_lam;

    % Gap between conductors.
motor.geom.k_winding = 1 -((motor.geom.C_g*
    motor.geom.C_l*motor.geom.q*motor.el.N_ph*
    motor.variables.Np)/(pi*((motor.variables.C_DO
    /2)^2-(motor.geom.C_DI/2)^2)));  % Fill factor (
    slotless), C_g = mellomrom mellom ledere, C_l =
    lenge av rett omrde p  leder, q*ph*p=N_s
motor.geom.w_s = (motor.geom.tau_s*motor.geom.r_avg)
    -motor.geom.w_lam;                      % gap
    between slots

motor.geom.C_w_avg = 2*motor.geom.r_avg*tan(
    motor.geom.tau_s/2)*(1-motor.geom.R_iron);  %
    Average conductor width. (straight area)
motor.el.alpha_slot = 2*pi*motor.variables.Np/2/
    motor.geom.Ns;                          % Slot
    angle [rad]

%% coefficients %%

motor.geom.k_c = (1-(2*motor.geom.w_s/(pi*
    motor.geom.tau_s))*(atan(motor.geom.w_s/
    motor.variables.g))-(motor.variables.g/(2*
    motor.geom.w_s))*log(1+(motor.geom.w_s/
    motor.variables.g)^2))^-1;
% Carters coefficient from (ref hanselmannn)

motor.geom.tau_c = motor.geom.tau_p;
motor.geom.k_p = motor.geom.tau_c/motor.geom.tau_p;
                    %Pitchin factor, k_p = tau_c/
    tau_p, tau_c = tau_p, theta_ce = pi osv osv
motor.geom.theta_se = pi/(motor.geom.q*motor.el.N_ph
    );              % Slot pitch
motor.geom.k_d = sin(motor.geom.q*
    motor.geom.theta_se/2)/(motor.geom.q*sin(
    motor.geom.theta_se/2)); % Distribution factor =
     1
motor.geom.k_w = motor.geom.k_p*motor.geom.k_d;
                    % Winding factor = 1 because
     of q = 1;

%% Reluctances and permeances per meter radial
    length %%

motor.mag.R_pm = motor.variables.M_d/(
    motor.constant.my_0*motor.geom.M_w);
                        % Permanent magnet
    reluctance. Only half of the width.
motor.mag.R_g = motor.variables.g*motor.geom.k_c/(
    motor.constant.my_0*motor.geom.M_w);          %
    Air gap reluctance. Half magnet width.
motor.mag.R_s = motor.geom.L_alength/(
    motor.constant.my_0*motor.constant.my_iron*
    motor.geom.w_lam); % Slot permeance, w_lam =
    Lamination with width and L_alength = Lamination
     length axially
motor.mag.R_ml = ((motor.constant.my_0/pi)*log(1+pi*
    motor.variables.g/(motor.geom.tau_p-
    motor.geom.tau_m)))^-1;
motor.mag.R_ml = real(motor.mag.R_ml);

    % Because R_ml might become imaginary
motor.mag.R_mr = (motor.constant.my_0/pi*log(1+(pi*
    min(motor.variables.g,(motor.geom.tau_p-
    motor.geom.M_w)/2)/motor.variables.M_d)))^-1;
                    % leakage from magnet to rotor
motor.mag.R_l = motor.geom.w_s/(motor.constant.my_0
    *(1/2)*motor.geom.L_alength);                 %
    Leakage reluctance between stator teeth
motor.mag.R_m = (2*motor.mag.R_pm)*motor.mag.R_mr
    /((2*motor.mag.R_pm)+motor.mag.R_mr);         %
     Parallel reluctance of 2*R_pm and R_mr

motor.mag.R_1 = motor.mag.R_ml*2*motor.mag.R_m/(
    motor.mag.R_ml+(2*motor.mag.R_m));
    % Parallel reluctance of 2*R_m and R_ml
motor.mag.R_2 = ((4*motor.mag.R_g)+motor.mag.R_1)*
    motor.mag.R_l/((4*motor.mag.R_g)+motor.mag.R_1+
    motor.mag.R_1); % Parallel reluctance of (4R_g+
    R_1) and R_l

motor.mag.phi_m = motor.mag.Br*motor.geom.M_w;

    % Magnetic flux from magnet

motor.mag.phi_g = (motor.mag.R_1/(motor.mag.R_2+(4*
    motor.mag.R_g)+motor.mag.R_1))*motor.mag.phi_m;
     % Air gap flux
motor.mag.B_g = (motor.mag.R_1/(motor.mag.R_2+(4*
    motor.mag.R_g)+motor.mag.R_1))*motor.mag.Br;
          % Air gap flux density

%% El %%


motor.el.Iph_rms = motor.variables.J*
    motor.geom.C_w_avg*motor.variables.C_d*(1000^2);
fit = 0;
n_t = motor.variables.N_lay;
M = 0;

while fit==0

    M = M+1;
```

```
    L_s = (1/2)*(n_t^2)*motor.constant.my_0*
        motor.geom.L_alength*motor.geom.C_l/(
        motor.geom.w_s*3);                    %
        Inductance per slot Hanselmann
    L_g = (n_t^2)*motor.constant.my_0*motor.geom.C_l
        *motor.geom.tau_p/(4*(motor.variables.M_d+
        motor.variables.g));       % Airgap
        inductance per coil Hanselmann.
    L_es = ((n_t^2)*motor.constant.my_0*
        motor.geom.tau_p/8)*log((motor.geom.tau_p^2)
        *pi/(4*motor.geom.L_alength*motor.geom.w_s))
        ;   % End section leakage inductance
        approximation
    L_coil = 2*L_g+L_s+L_es;

        % Total inductance per coil. Hanselmann
    motor.el.L_ph = L_coil*motor.variables.Np;

        % Inductance of all coils in a series (1
        phase) N_p, eller N_p/2, eller N_s/2??

    R_active = (motor.geom.C_l/(
        motor.constant.sigma_alu*motor.geom.C_w_avg*
        motor.variables.C_d))*motor.variables.Np*n_t
        *motor.geom.q;
                                              %
        Resistance of active coil (Pr phase)
    R_es_upper = (6*motor.geom.tau_s*(
        motor.variables.C_DO/2)/(
        motor.constant.sigma_alu*motor.geom.C_w_avg
        *(motor.variables.C_d/2)))*(
        motor.variables.Np/2)*n_t*motor.geom.q; %
        Resistance of upper end section (Pr phase)
    R_es_lower = (6*motor.geom.tau_s*(
        motor.geom.C_DI/2)/(motor.constant.sigma_alu
        *motor.geom.C_w_avg*(motor.variables.C_d/2))
        )*(motor.variables.Np/2)*n_t*motor.geom.q;
             % Resistance of lower end section (Pr
        phas)

    motor.el.E_ph_rms      = (1/sqrt(2))*
        motor.el.omega_e*motor.geom.q*n_t*
        motor.geom.q*motor.mag.B_g*motor.geom.tau_p*
        motor.geom.r_avg*motor.geom.C_l*(
        motor.variables.Np/2)*M;
                          % RMS induced phase
        voltage
    motor.el.R_loss        = R_active+R_es_upper+
        R_es_lower;

        % Resistance equivalent for the total
        electrical losses.
    motor.el.V_R_ph_rms    = motor.el.Iph_rms*
        motor.el.R_loss;

        % Active RMS voltage drop
    motor.el.V_X_ph_rms    = motor.el.Iph_rms*
        motor.el.omega_e*motor.el.L_ph;
                                              %
        Reactive RMS voltage drop
    motor.el.V_ph_rms  = sqrt((motor.el.E_ph_rms+
        motor.el.V_R_ph_rms)^2 + motor.el.V_X_ph_rms
        ^2);                    % Terminal RMS phase
         voltage
    motor.el.V_ll_rms      = sqrt(3)*
        motor.el.V_ph_rms;

        % Terminal RMS line voltage
    motor.el.S_base = sqrt(3)*motor.el.V_ll_rms *
        motor.el.Iph_rms;

    if M == 0
        M = 1;
    end
    if motor.el.E_ph_rms >=motor.el.Eph_req
        fit=1;
                % Quit while-loop
        end
    end

    motor.geom.M = M;
    motor.mech.T = motor.geom.M*motor.variables.C_d*
        motor.variables.Np*motor.mag.B_g*
        motor.variables.N_lay*motor.geom.q*2*sqrt(2)*
        motor.variables.J*motor.geom.C_w_avg*cos(pi/6)*
        motor.geom.C_l*motor.geom.r_avg*1000^2;
    motor.el.cos_phi = (motor.el.E_ph_rms+
        motor.el.V_R_ph_rms)/motor.el.V_ph_rms;

    %% Calculation of mass %%

    % Stator Lamination

    motor.mech.V_laminations = motor.geom.w_lam*
        motor.geom.L_alength*motor.geom.L_lam*
        motor.geom.Ns;     % [m^3] stator lamination
        volume
    motor.mech.M_laminations = (motor.mech.V_laminations
        )*motor.constant.rho_lamination*motor.geom.M; %
        [kg] Weight of laminations

    % Conductors
    motor.mech.V_c_active = motor.geom.C_l*
        motor.geom.C_w_avg*motor.variables.C_d*
        motor.variables.N_lay*motor.geom.Ns;
                                    % Volume of active
        conductors
    motor.mech.V_es_upper = 6*motor.geom.tau_s*(
        motor.variables.C_DO/2)*motor.geom.C_w_avg*(
        motor.variables.C_d/2)*motor.variables.N_lay*(
        motor.geom.Ns/2); % Upper end coil volume
    motor.mech.V_es_lower = 6*motor.geom.tau_s*(
        motor.geom.C_DI/2)*motor.geom.C_w_avg*(
        motor.variables.C_d/2)*motor.variables.N_lay*(
        motor.geom.Ns/2);    % Inner end coil volume
    motor.mech.V_conductor = (motor.mech.V_es_upper +
        motor.mech.V_es_lower + motor.mech.V_c_active)*
        motor.geom.M;                       % [m^3] volume
         of conductors (fill factor osv)

    motor.mech.M_conductor = motor.mech.V_conductor*
        motor.constant.rho_alu;  % [kg] Weight of
        conductors

    % Magnets

    motor.mech.V_pm = (motor.variables.M_d*
        motor.geom.M_l*motor.geom.M_w)*
        motor.variables.Np*2*motor.geom.M;              %
         [m^3] Magnet volume (2 Rotor discs)
    motor.mech.M_pm = motor.mech.V_pm*
        motor.constant.rho_pm;
                                                  % [kg
        ] Weight of PM's

    % Rotor  Steel (Back Iron)

    motor.mech.V_BI = (2*motor.geom.BI_D*(((
        motor.geom.M_DO/2)^2)-((motor.geom.M_DI/2)^2))*
        pi);   % [m^3] Back Iron Volume (2 rotor discs)
    motor.mech.M_BI = motor.mech.V_BI*
        motor.constant.rho_steel;
                                       % [kg] Weight of
         back iron

    % Housing and shaft approximations.

    motor.mech.M_totL = motor.geom.M*(
        motor.geom.L_alength+(2*(motor.variables.g+
        motor.variables.M_d+motor.geom.BI_D)));         %
         Total machine length
    motor.mech.V_shaft = (((((motor.geom.C_DI/4)+(
        motor.mech.Shaft_d/2))/2)^2)-((((motor.geom.C_DI
```

```
    /4)-(motor.mech.Shaft_d/2))/2)^2))*pi*
    motor.mech.M_totL; % Shaft volume
motor.mech.M_shaft = motor.constant.rho_steel*
    motor.mech.V_shaft;
                                        % Shaft
    weight

motor.mech.D_housing = motor.variables.C_DO
    +(10/1000);
                                       % Housing
    inner diameter
motor.mech.V_housing = (motor.mech.M_totL/
    motor.geom.M)*pi*((((motor.mech.D_housing
    +(20/1000))/2)^2)-((motor.mech.D_housing/2)^2));
motor.mech.M_housing = motor.constant.rho_steel*
    motor.mech.V_housing;


%% Cost calculation %%

motor.cost.laminations = motor.mech.M_laminations*
    motor.cost.C_laminations;   % [Euro  ]
    Lamination material cost
motor.cost.PM = motor.mech.M_pm*motor.cost.C_pm;
                                % [Euro  ]
    Permanent magnet material cost
motor.cost.conductors = motor.mech.M_conductor*
    motor.cost.C_aluconductor;     % [Euro  ]
    Conductor material cost
motor.cost.BI = motor.mech.M_BI*motor.cost.C_steel;
                            % [Euro  ] Back iron
    material cost
motor.cost.Shaft = motor.mech.M_shaft*
    motor.cost.C_steel;                     % [Euro
     ] Shaft material cost
motor.cost.Housing = motor.mech.M_housing*
    motor.cost.C_steel;                 % [Euro  ]
    Housing material cost

%% Losses %%

% Conductor resistance pr M

motor.el.R_active = (motor.geom.C_l/(
    motor.constant.sigma_alu*motor.geom.C_w_avg*
    motor.variables.C_d))*motor.variables.Np*
    motor.variables.N_lay*motor.geom.q;
                                        %
    Resistance of active coil (Pr phase)
motor.el.R_es_upper = (6*motor.geom.tau_s*(
    motor.variables.C_DO/2)/(
    motor.constant.sigma_alu*motor.geom.C_w_avg*(
    motor.variables.C_d/2)))*(motor.variables.Np/2)*
    motor.variables.N_lay*motor.geom.q; % Resistance
     of upper end section (Pr phase)
motor.el.R_es_lower = (6*motor.geom.tau_s*(
    motor.geom.C_DI/2)/(motor.constant.sigma_alu*
    motor.geom.C_w_avg*(motor.variables.C_d/2)))*(
    motor.variables.Np/2)*motor.variables.N_lay*
    motor.geom.q;      % Resistance of lower end
    section (Pr phas)

motor.el.R_DC = motor.geom.M*(motor.el.R_active +
    motor.el.R_es_upper + motor.el.R_es_lower); %
    Total DC resistance pr phase.

% DC losses

motor.el.P_DC = motor.el.R_DC*motor.el.N_ph*(
    motor.el.Iph_rms^2);

% AC losses

motor.el.delta = sqrt(2/(motor.el.omega_e*
    motor.constant.my_0*motor.constant.sigma_alu));
motor.el.R_ec = (motor.geom.L_alength*motor.geom.C_l
    *(motor.variables.C_d^2)*(motor.variables.N_lay
    ^2)/(9*motor.constant.sigma_alu*(motor.el.delta
    ^4)*motor.geom.w_s));
motor.el.P_ec = motor.el.R_ec*motor.el.Iph_rms*
    motor.geom.Ns*motor.geom.M;

% Efficiency

motor.el.efficiency = ((motor.mech.T*
    motor.mech.omega_m)/(sqrt(3)*motor.el.V_ll_rms*
    motor.el.Iph_rms);

%% Objective function %%

motor.mech.M_weight = (motor.mech.M_laminations +
    motor.mech.M_conductor + motor.mech.M_pm +
    motor.mech.M_BI+motor.mech.M_shaft+
    motor.mech.M_housing); % [kg] total weight of
    machine
motor.cost.mech = motor.cost.laminations +
    motor.cost.PM + motor.cost.conductors +
    motor.cost.BI+motor.cost.Housing+
    motor.cost.Shaft; % [Euro  ] Material cost of
    machine

motor.el.E_loss_yearly = (motor.el.P_DC+
    motor.el.P_DC)*(3600/1000)*motor.mech.time_fullP
    ;
motor.cost.E_loss_yearly = motor.el.E_loss_yearly*
    motor.cost.E_price;
motor.cost.E_total = 0;

for k=1:motor.constant.lifetime
    motor.cost.E_total = motor.cost.E_total + (
        motor.cost.E_loss_yearly/((1+
        motor.cost.disc_rate)^k));
end

motor.cost.total = motor.cost.E_total +
    motor.cost.mech;

% f = [];
% f = motor.cost.total;
% f = motor.mech.M_weight;
f = motor.cost.mech;

 %% Inequality constraints %%

c = [
    (motor.el.f-lim_f)*0.01;
                                          % f <=
        lim_f
     (-motor.mech.T+motor.mech.T_req)/1000;
                              % T >= T_req
    -motor.geom.w_lam+lim_tooth;
                                       % w_lam >=
        lim_tooth
    -motor.geom.C_w_avg;
                                             % C_W
        >= 0
    -motor.geom.r_I;
                                                %
        R_inner >= 0
     (-motor.el.E_ph_rms+motor.el.Eph_req)*0.001;
                      % Eph > Eph_req
     real(-motor.el.cos_phi+Lim_PF);
                                    % Cos(phi)> Lim_pf
     (motor.geom.R_iron-Lim_Riron)
                                     % R_iron =< 0.9
    ];

%% Equality constraints %%

ceq = [];
```